

Thermosetting Allyl Resins Derived from Soybean Fatty Acids

Qiang Luo, Min Lui, Yijin Xu, Mihail Ionescu, Zoran S. Petrovic

Kansas Polymer Research Center, Pittsburg State University, Pittsburg, Kansas 66762

Correspondence to: Q. Luo (E-mail: qiangluo2005@gmail.com)

ABSTRACT: A novel class of thermosetting resins based on allylated and transesterified epoxidized soybean oil (AE-ESBO) curable by radical mechanism was developed. The AE-ESBO was prepared from ESBO by oxirane ring-opening and then transesterification with allyl alcohol. A family of rubbery to glassy resins was prepared by radical copolymerization of AE-ESBO with different concentrations of maleic anhydride (MA). Glass transition temperatures (T_g) of these resins ranged from below room temperature to about 130°C based on the amount of MA. In spite of the presence of anhydride groups, water absorption was low <2% even when maleic anhydride was 30% of total weight. Low sol content after extraction and low swelling in toluene indicated high crosslinking density. Tensile moduli of these resins were up to 1.4 GPa and tensile strengths up to 37 MPa. © 2012 Wiley Periodicals, Inc. *J. Appl. Polym. Sci.* 000: 000–000, 2012

KEYWORDS: plant oil; allyl polymers; thermo-mechanical properties

Received 9 January 2012; accepted 14 March 2012; published online

DOI: 10.1002/app.37814

INTRODUCTION

Plant oil-based materials are becoming increasingly attractive because of environmental concerns, novel properties and economics. Great efforts have been endowed into this area by scientific and industrial researchers in recent years. Plant oils are triglycerides, that is, three fatty acids are chemically bonded with glycerol through ester bond. Three major unsaturated fatty acids in soybean oil are oleic, linoleic, and linolenic. The internal double bonds in plant oils are inert to free radical polymerization. Cationic polymerization catalyzed with Lewis acids or superacids, could only result in low molecular weight oligomers or soft rubbers.^{1–6} Low molecular weight oligomer oils were also the best results by polymerization of metathesis.⁷ To get solid products with useful engineering properties, other functional monomers are usually adopted for copolymerization. Promising methods of making solid polymers from biobased triglycerides are modifying plant oils into polyols, polyacids or polyamines and reacting them with other monomers to produce polyurethanes, polyureas or polyesters.^{8–15} These methods unfortunately involved multistep synthesis, low biomass content, utilization of toxic and expensive reactants such as isocyanates and sometimes loss of useful properties, such as increasing dielectric constant and dielectric loss compared to the starting oils. The ideal modification of vegetable oil systems should allow direct polymerization to

polymeric products at low capital cost and with high biomass content.

So far free radical polymerization was investigated on acrylated oils prepared from epoxidized vegetable oils or fatty acids.^{16–25} Here at Kansas Polymer Research Center, novel allylated epoxidized soybean oil (ESBO) with lateral double bonds was developed and reported.²⁶ Derived from this modified plant oil, a variety of novel thermosetting materials ranging from elastomers to tough, rigid plastics were prepared. The objective of this work was to further improve the properties of those materials using fatty acid monomers instead of triglycerides. The novel monomer was obtained by transesterification of allylated epoxidized oil with allyl alcohol to increase double bond concentration and to significantly increase modulus and tensile strength of thermosetting resins. The resins were prepared by copolymerization with maleic anhydride (MA).

EXPERIMENTAL

Materials

Dicumyl peroxide (DCP), tetrafluoroboric acid (54 wt %) in ether, and Di-tert-butyl peroxide (t-BP) (98%) were purchased from Aldrich (Milwaukee, WI). MA was purchased from Acros Organic (Morris Plains, NJ). Allyl alcohol (99%) was purchased from Alfa Aesar (Ward Hill, MA). Anhydrous magnesium sulfate, tetrahydrofuran, toluene, and methylene chloride were

obtained from Fisher Scientific (Pittsburgh, PA). ESBO was obtained from American Chemical Service (Griffith, IN). Mold release agent E155 was obtained from Wacker Chemical Corp. (Adrian, MI). Potassium methoxide was obtained from Sybron Chemical (Torrance, CA). All chemicals were used as received except that ESBO was filtered before use.

Measurements

Hydroxyl numbers were determined according to ASTM D 1957-86.

Fourier transform infrared (FTIR) spectroscopy was recorded on a Perkin-Elmer, Waltham, MA. Spectrum-1000 FTIR spectrometer, scanning from 500 to 4000 cm^{-1} .

Proton nuclear magnetic resonance was performed on a Bruker Advance DPX-300 spectrometer at 300 MHz with a 5-mm broadband probe. Deuterated chloroform was used as solvent.

A thermogravimetric analyzer model Q50 (TA Instruments) was used for examining thermal stability of cured resins. Calibration and experiments were performed under the nitrogen gas with a heating rate of 10°C/min from room temperature up to 600°C.

Dynamic mechanical analysis was performed on DMA 2980 from TA Instruments with extension mode, at 1 Hz, and at a heating rate of 2°C/min in a temperature range between -90 and 250°C with amplitude of 15 μm .

Gel permeation chromatography (GPC) was found to be well-suited to follow the formation of dimers or trimers during oil molecule modifications. Waters GPC model 510, equipped with 4 Phenomenex columns covering molecular weight range 100–1,000,000 and differential refractometer model 410 (Waters, Milford, MA), with tetrahydrofuran as the eluent was used to follow the molecular weight variation. The flow rate of tetrahydrofuran was 1 mL/min at room temperature.

Viscosity was measured on an AR 2000 dynamic stress rheometer from TA Instruments with cone plate, New Castle, DE at 25°C with cone plates of 25 mm in diameter, having a gap of 55 μm .

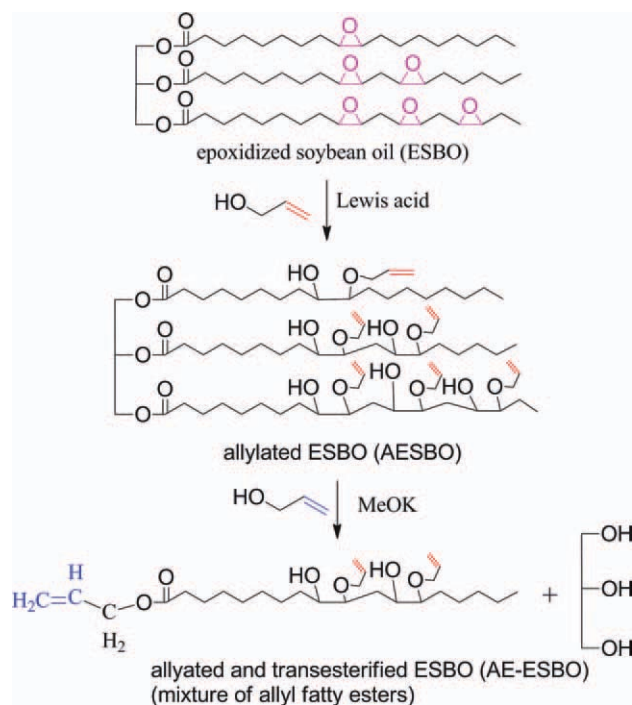
Tensile properties were measured according to ASTM D882-01 using a tensile tester model 4467 from Instron, Canton, MA.

Epoxy oxygen content (EOC) determination was performed according to the standard procedure for oils and fats.²⁷

Iodine value (IV) was determined by the Hanus method.²⁸

ASTM D570 was followed to measure water absorption of cured resins by immersing cured resins in water at 23°C for 24 h. Specimens were taken out and both of the surfaces were dried with paper before weighing. Water absorption was calculated from the difference in the weights of the swollen and dry sample.

ASTM D543 was followed to measure swelling ratio of cured resins by immersing cured resins in toluene at 23°C. Specimens were taken out and both of the surfaces were dried with paper before weighing every 24 h until weight equilibrates. The swelling ratio was calculated from the difference in equilibrium weights of the swollen and dry sample.



Scheme 1. Preparation of AE-ESBO. [Color figure can be viewed in the online issue, which is available at wileyonlinelibrary.com]

Gel content of cured resins was determined with Soxhlet extraction. Specimens of 3–5 mm long and about 1-mm thick were cut from bulk resins and were extracted with 100 mL of refluxing methylene chloride using a Soxhlet extractor until the dry weight of resins did not change (24 h is enough in all of the cases). The extracted materials were then dried in vacuum oven at 100°C for 1 h. Gel content was calculated from the difference in weight of the dry samples before and after extraction.

Density of cured resins was measured by immersing in water according to ASTM 792-08.

Synthesis of Allylated and Transesterified ESBO

allylated and transesterified ESBO (AE-ESBO) was synthesized by a one pot two-step process. Scheme 1 illustrates the synthetic pathway. A typical reaction is as follows: the prescribed amount of allyl alcohol was mixed with catalyst tetrafluoroboric acid (0.5 wt % of total weight) in a three-neck round flask which was equipped with a magnetic stirrer, nitrogen inlet and outlet, and an addition funnel. The flask was heated in an oil bath. After the temperature reached 80°C, predetermined amount of ESBO was added into the flask dropwise. Molar ratio of allyl alcohol to epoxy groups in ESBO was 6–8. After all the ESBO was added, the EOC of the reaction mixture was tracked by standard measurement procedures for oils and fats. When EOC is not detectable, potassium methoxide (1 wt % of ESBO) was added in excess to neutralize acid catalyst and to catalyze transesterification at 80°C for 1 h. Excess allyl alcohol was removed and recycled with a rotary evaporator. The crude oil was then washed in a separation funnel with distilled water three times to get rid of triglycerol and allyl alcohol. The oil layer was then dried with anhydrous magnesium sulfate.

Table I. Properties of AE-ESBO and ESBO

Oil ID	Viscosity (Pa s)	IV	OH# (mg KOH/g)	EOC (%)
ESBO	0.41	1.0	5.0	7.0
AE-ESBO	0.09	108	182	0.02

Preparation of AE-ESBO-co-MA Resins

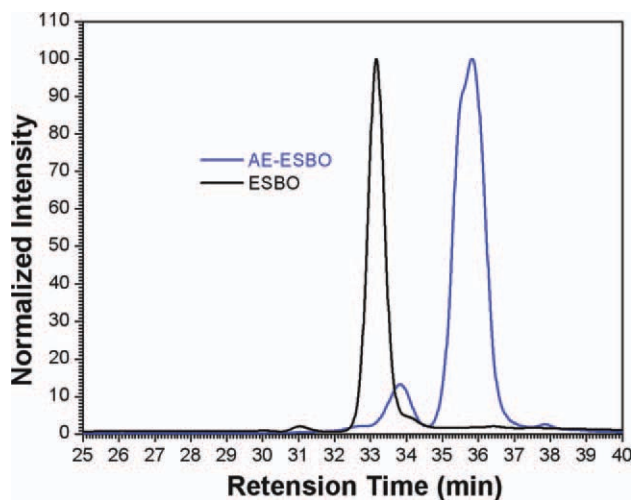
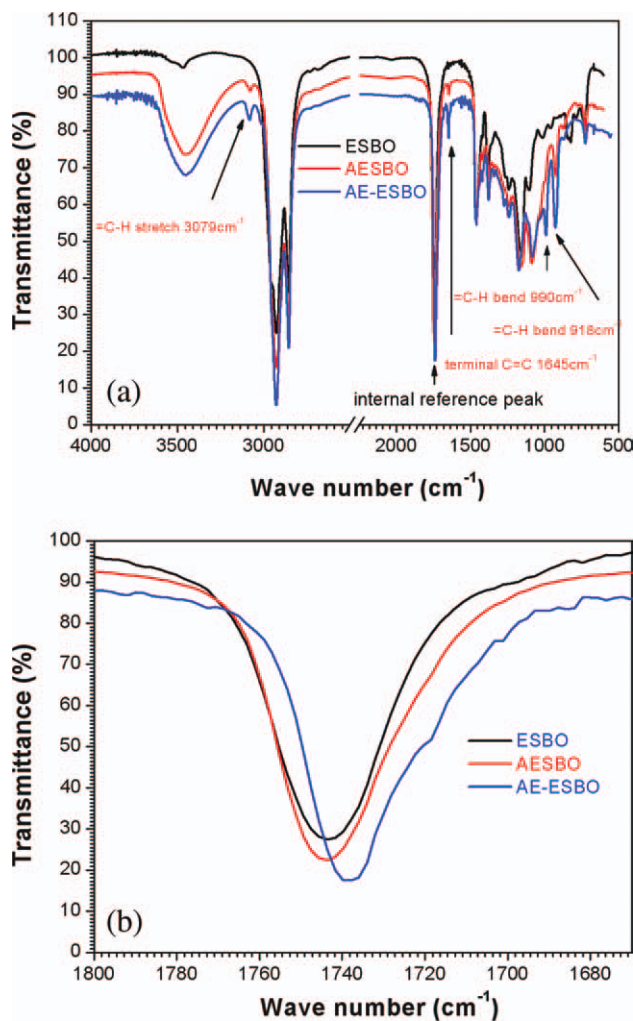
Calculated amount of AE-ESBO, MA, and DCP were mixed in a 25 mL vial sealed with rubber stopper. The mixture was vacuumed to eliminate dissolved water and gas and then heated to $\sim 120^{\circ}\text{C}$. The reaction was brought to atmospheric pressure with nitrogen gas. The mixture was stirred with magnetic stirrer until viscosity was high enough (vortex almost disappeared). A lot of gas bubbles were produced during this process. Vacuum was applied to eliminate the bubbles. The pressure was again increased to atmosphere pressure with nitrogen gas. The viscous mixture was then poured into a hot mold under nitrogen atmosphere to cast $100 \times 100 \times 1 \text{ mm}^3$ sheets. The mold was then heated in oven at 120°C for 2 days.

RESULTS AND DISCUSSION

Synthesis and Characterization of AE-ESBO Monomer

As in our published paper, allylated ESBO (AESBO) had relatively low IV.²⁶ Material properties were theoretically compromised due to the relatively high double bond equivalent weight. To increase the double bond concentration, the AESBO was further modified by transesterification with excess of allyl alcohol to produce fatty esters of allyl alcohol (AE-ESBO). The measured OH number and EOC in Table I is the same as with AESBO.²⁶ IV was increased to 108 g I₂/100 g oil, (IV can be expressed in percentage or without units) which is very close to the theoretical value of 109.7 g I₂/100 g oil based on IV of AESBO.²⁶

After transesterification, triglycerides become fatty esters. Because molecular weight of a fatty ester is about one third of that of triglycerides, the main peak of AE-ESBO shifted to a longer retention time in GPC, as shown in Figure 1. The asymmetric main peak of AE-ESBO around 35.8 min demonstrated

**Figure 1.** GPC chromatography of ESBO and AE-ESBO. [Color figure can be viewed in the online issue, which is available at wileyonlinelibrary.com]**Figure 2.** FTIR spectra of AE-ESBO (blue), AESBO (red), and ESBO (black). [Color figure can be viewed in the online issue, which is available at wileyonlinelibrary.com]

the existence of fatty esters of close but different molecular weights due to different amount of double bonds. It is the result of coexistence of oleic, linoleic, and linolenic fatty ester moieties. These three unsaturated fatty esters have one, two, and three double bond(s) in their molecules, respectively. After epoxidation, double bonds became epoxy rings. When those epoxy rings were opened with allyl alcohol, theoretical molecular weight increase was 58, 116, and 174 g/mol, respectively. The allyl ester of these ring-opened compounds should have molecular weight of about 396, 452, and 508 g/mol. The resolution of GPC could not separate these three allylated fatty esters and resulted asymmetric peak is due to a partially peak overlap. Just as in AESBO, GPC also indicated the existence of the dimers and other oligomers in AE-ESBO due to the competition between primary allyl alcohol and the secondary alcohol produced in ring-opening.

The ester peak around 1742 cm^{-1} in the FTIR spectrum was taken as the internal reference and other peaks were normalized to it since ester concentration did not change significantly before and after transesterification. FTIR spectra in Figure 2(a)

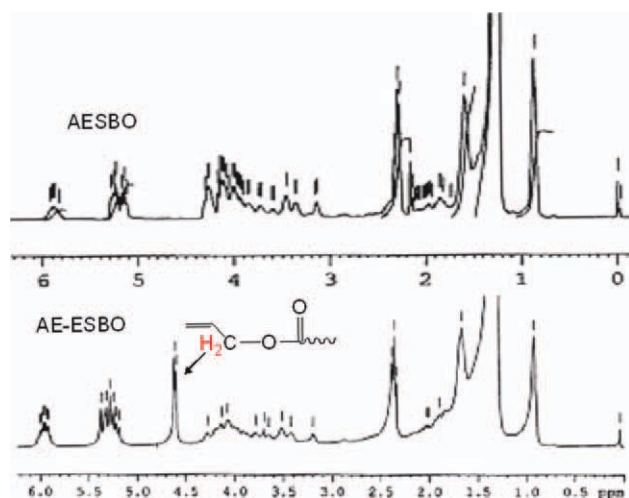


Figure 3. $^1\text{H-NMR}$ of AESBO and AE-ESBO. [Color figure can be viewed in the online issue, which is available at wileyonlinelibrary.com]

display a much stronger peak at 3079 cm^{-1} assigned to $=\text{C}-\text{H}$ stretching in terminal double bond, at 1645 cm^{-1} assigned to $-\text{C}=\text{C}-$ stretching in terminal double bond. The peak at 921 cm^{-1} is assigned to $=\text{C}-\text{H}$ bending in terminal double bond, which indicated higher concentration of double bonds in AE-ESBO molecules.²⁹ Peak around 990 cm^{-1} also assigned to $=\text{C}-\text{H}$ bending in terminal double bond which only showed a small shoulder in the FTIR spectrum of AESBO.²⁹ The peak was much stronger and more obvious in the FTIR spectrum of AE-ESBO in Figure 2. It is another indicator of higher concentration of terminal allyl double bond in AE-ESBO than AESBO. Although the ester concentration did not change after transesterification, when triglycerides were transesterified to allyl esters, the peak position of ester shifted from 1744 to 1738 cm^{-1} due to dipole variation after transesterification, as shown in Figure 2(b).

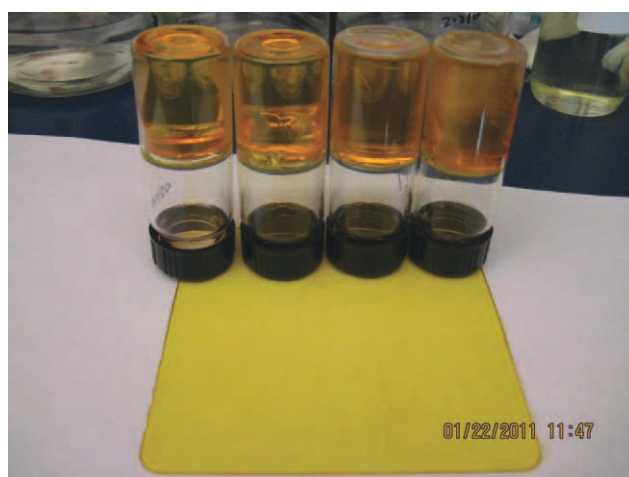


Figure 4. Cured AE-ESBO-co-MA resin. MA loading from left to right: 30, 20, 15, and 10 wt %. The sheet contains 30 wt % of MA. [Color figure can be viewed in the online issue, which is available at wileyonlinelibrary.com]

Table II. Properties of AE-ESBO-co-Maleic Anhydride

Polymerized at 120°C	Gel content (%)	Swelling (%)	H_2O absorption (%)	Density (10^3kg/m^3)
AE-ESBO + MA 10%	89.0	34.5 (2 days)	1.3	1.07 ± 0.01
AE-ESBO + MA 15%	96.3	27.9 (2 days)	1.4	1.09 ± 0.01
AE-ESBO + MA 20%	96.3	21.6 (2 days)	1.3	1.12 ± 0.01
AE-ESBO + MA 30%	96.4	12.9 (7 days)	1.4	1.20 ± 0.02
AE-ESBO + MA 40%	88.8	4.2 (4 days)	1.8	1.16 ± 0.01

During transesterification, allyl alcohol replaced glycerol to form ester bond with fatty acid. The allyl proton ($\alpha\text{-CH}_2$) to double bond in esters have different chemical environment than those in allyl ether. They should give a different peak in $^1\text{H-NMR}$. In Figure 3, a peak around 4.7 ppm observed in $^1\text{H-NMR}$ of AE-ESBO, which is assigned to allyl protons ($\alpha\text{-CH}_2$) to double bond in the ester, is absent in that of AESBO. Because of the overlap of methine ($-\text{CH}-$) in glycerol moiety and methylene ($=\text{CH}_2$) in double bonds around 5.2 ppm and the overlap of methylene hydrogens in glycerol moiety and peaks of the side reaction products of cyclic ether around 4.2 ppm,^{26,30,31} it is hard to tell by $^1\text{H-NMR}$ whether there is a significant triglyceride residue. Fortunately, GPC and IV before and after transesterification demonstrated that even if there was a triglyceride residue, the amount is not significant.

Effects of MA Loadings

AE-ESBO was copolymerized with different amount of MA to study the effect of MA loading on properties of cured resins. Cured resins with different MA loadings in cylinder form and sheet are shown in Figure 4. The color of sheet form material is lighter than the cylindrical material. This is the cross check of our explanation in our previous paper.²⁶

As t-BP was adopted when AESBO triglyceride was copolymerized with MA, the same amount of t-BP (6 wt %) was also attempted to initiate copolymerization of AE-ESBO and MA. Unfortunately, the reaction was so violent that reaction happened in few seconds after the injection of t-BP. The reaction was still too violent to control even at 1 wt % of t-BP. The violent reaction may result from relatively higher double bond concentration in AE-ESBO and low boiling point of t-BP. High boiling point free radical initiator was chosen as a potential alternative. DCP has boiling point of 351°C and 10-h half-life time at 116°C . As already known in curing AESBO and MA, 6 wt % of initiator gave the best properties.²⁶ The same amount of DCP (6 wt %) was applied to cure AE-ESBO and MA.

The ultimate swelling ratios of copolymer resins are presented in Table II. Higher polar MA loading in resins resulted in lower swelling ratios. Decreased swelling ratios from ~ 35 to $\sim 4\%$ were observed when MA loading increased from 10 to 40 wt %.

Table III. Tensile Properties of AE-ESBO-*co*-Maleic Anhydride

	Bio-content (%)	Young's modulus (MPa)	Tensile strength (MPa)	Elongation at break (%)
AE-ESBO + MA 10%	62.7	13.2 ± 0.4	1.1 ± 0.2	10.4 ± 1.7
AE-ESBO + MA 15%	59.2	150 ± 21	5.0 ± 0.9	5.5 ± 1.0
AE-ESBO + MA 20%	55.8	673 ± 24	17.6 ± 1.5	4.9 ± 1.2
AE-ESBO + MA 30%	48.8	1452 ± 28	37.3 ± 1.5	4.2 ± 0.5
AE-ESBO + MA 40%	41.8	863 ± 56	23.6 ± 1.6	6.1 ± 1.2

During the test, all of the specimens reached swelling equilibrium in 2 days except the specimens of resins containing 30 wt % of MA, which took 7 days to reach equilibrium and the one containing 40 wt % of MA, which took 4 days to equilibrate. When MA loading was less or equal to 20 wt %, the swelling ratios of resins derived from AE-ESBO were lower than that derived from AESBO. However, when MA was 30 wt %, the resin derived of AE-ESBO showed higher swelling ratio than that derived from AESBO initiated with t-BP. For double check, swelling of these two resins in toluene was conducted twice under same conditions. The results were consistent.

ASTM D570 was adopted for water absorption measurement. Data in Table II showed that water absorption of copolymer resins was less than 2% and was independent of MA loadings. The water absorption of resins derived of AE-ESBO was about 50% higher than that of the counterparts derived from AESBO.

Table II shows that gel content measured by Soxhlet extraction increased from 89 to 96% when MA loading increased from 10 to 30 wt %, which indicates higher crosslinking density. Further

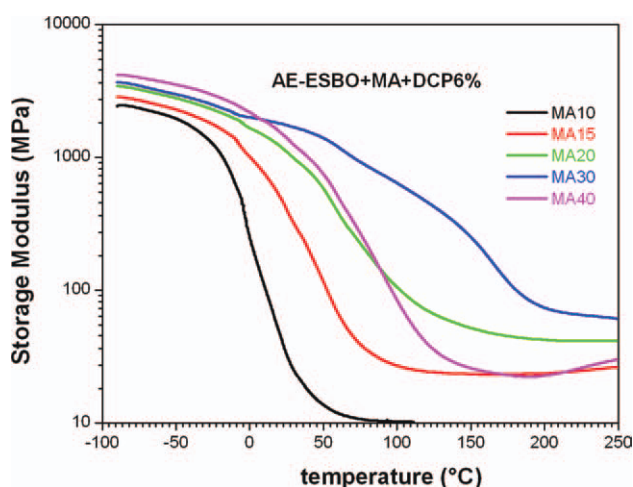


Figure 5. Storage modulus of AE-ESBO-*co*-MA with different MA content. (black: 10 wt %, red: 15 wt %, green: 20 wt %, blue: 30 wt %, magenta: 40 wt %). [Color figure can be viewed in the online issue, which is available at wileyonlinelibrary.com]

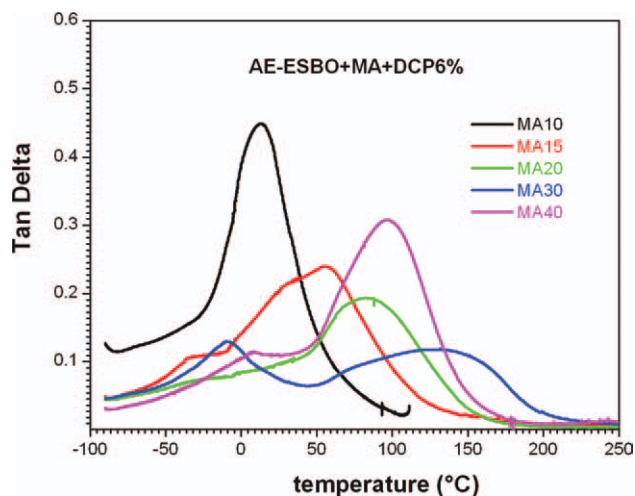


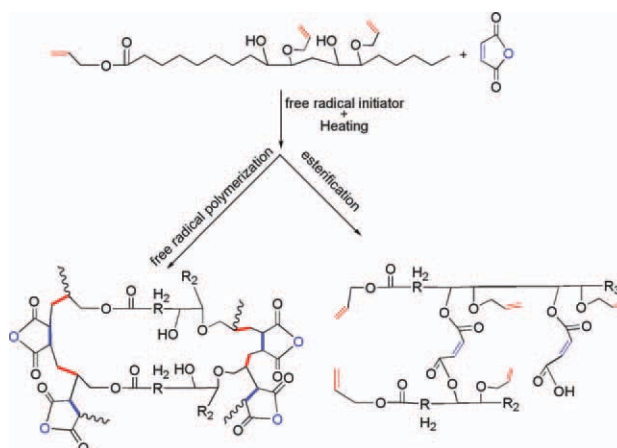
Figure 6. Tan δ of AE-ESBO-*co*-MA with different MA loadings. (black: 10 wt %, red: 15 wt %, green: 20 wt %, blue: 30 wt %, magenta: 40 wt %). [Color figure can be viewed in the online issue, which is available at wileyonlinelibrary.com]

increasing of MA loading to 40 wt % resulted in lower gel content. As prescribed in,²⁶ too much MA will decrease crosslinking density and lower gel content.

Biomass content (soy oil moiety) in Table III decreased with the increase of malein anhydride loading. When MA loading is 30 wt %, bio-content is a little less than 50 wt %.

Dynamic Mechanical Analysis

The dynamic mechanical analysis results in Figures 5 and 6 showed that the storage modulus in the glassy state of AE-ESBO-*co*-MA copolymers increased with increasing MA loading. In the rubbery state, storage moduli increased when MA increased from 10 to 30 wt %. Further increase to 40 wt % decreased rubbery storage modulus. At 10 wt % MA loading, the copolymer was too weak and broke prematurely. When MA loading was 15 wt %, rubbery storage modulus increased slightly upon heating, possibly due to shrinking above T_g or



Scheme 2. Reactions between AE-ESBO and MA. [Color figure can be viewed in the online issue, which is available at wileyonlinelibrary.com]

further curing. No detectable further thermal curing was observed when MA was 20 and 30 wt %. Interestingly, more thermal curing was observed at 40 wt % MA loading. It is very possible due to the dehydration of excessive carboxylic acid at high temperature.

Alpha transition temperature variation of the copolymer resins as measured by $\tan \delta$, displayed the same trend as the variation of rubbery storage moduli, that is, $\tan \delta$ peaks shifted to higher temperatures when MA loading increased from 10 to 30 wt %. Broad $\tan \delta$ peaks in samples with 30 and 40 wt % MA indicate a wide distribution of the molecular weights between crosslinking points as a consequence of the wide distribution of crosslinking densities. Most samples display a clear β -transition in the negative temperature region, tentatively assigned to the rotations of fatty acid segments. $\tan \delta$ peak of the copolymer with 40 wt % MA was between the peaks of copolymer with 20 and 30 wt % of MA. The lower glass transition temperature and lower rubbery storage modulus indicated lower crosslinking density of the copolymer. It is very possible the lower crosslinking density was due to the higher anhydride groups and non-stoichiometric amount of maleic double bond to allyl double bond. As shown in Scheme 2, two different reactions occurred during curing of AE-ESBO-*co*-MA copolymer. One is free radical polymerization of double bonds; the other is esterification of hydroxyl group and anhydride. When one anhydride group reacted with two hydroxyl groups to form two ester links, crosslinking occurs. If one anhydride only reacted with one hydroxyl group, one ester link and one free acid is produced, resulting in lower degree of crosslinking. However, free acid groups may form strong hydrogen bonds with hydroxyl groups contributing also to the cohesive strength of the material. It is well-known that when reacting with hydroxyl group,³² anhydride undergoes more easily than free acid does. Theoretically, free acid can react with hydroxyl groups only after anhydride groups are not available.

When MA was 30 wt %, by calculation, moles of allyl double bond in AE-ESBO was about the same with those of maleic double bond. As allyl double bond and maleic double form alternating polymer in free radical polymerization,³³ 30 wt % of MA is close to ideal mole ratio of two different double bonds. At the same time, mole numbers of anhydride is higher than that of hydroxyl group in the system. Any esterification between MA and hydroxyl group will increase crosslinking density no matter half ester or full ester formed. Full esterification of anhydride resulted higher crosslinking density than half ester. When MA content was 40 wt %, there is more maleic double bond than allyl double bond. There is even more anhydride group in excess to hydroxyl group than in case of 30 wt % of MA. It is well-known that there is almost no homopolymerization of maleic double bond. As a result, larger amount of incorporated MA formed half ester and free acid with unreacted maleic double bond. Also, relatively larger amount of unreacted MA was trapped in crosslinked resin, as indicated by lower gel content of resin with 40 wt % of MA.

The lower crosslinking density of the copolymer resin with 40 wt % of MA was also indicated by lower bulk density of the

resin compared to that of the resin with 30 wt % of MA, as shown in Table II. As MA has density of $1.48 \times 10^3 \text{ kg/m}^3$ while AE-ESBO density is lower than that of water. Resins with increasing density were achieved when MA loading increased up to 30 wt %. However, when increase MA loading to 40 wt %, density decreased to $1.16 \times 10^3 \text{ kg/m}^3$ from $1.20 \times 10^3 \text{ kg/m}^3$. So, the only possibility is the lower crosslinking density of the resin.

Mechanical Properties of AE-ESBO-*co*-MA

Tensile properties of AE-ESBO-*co*-MA resins were shown in Table III. Mechanical properties of polymers are strongly dependent of the physical state at the temperature of measurement. Whether our samples are glasses or rubbers at room temperature is determined by the glass transition temperature. Precise T_g values are usually obtained by DSC but the signals in our case were weak and no clear T_g were observed. T_g values from the $\tan \delta$ maxima may be shifted to higher temperature by as much as 20–50°C and are unreliable in predicting the physical state of our polymers at room temperature. Judging from modulus data it is clear that samples with 10 and 15 wt % MA are rubbery at room temperature while other were glassy.

The addition of MA up to 30 wt % increased the tensile strength and modulus of the resins due to crosslinking. Further increasing MA loading to 40 wt % gave a much weaker material. Low elongation at break of rubbery samples (with 10 and 15 wt % MA) suggests that they are poor rubbers possibly due to inhomogeneous crosslinking. Highly crosslinked polymers (30 and 40 wt % MA) had low elongations, characteristic of brittle materials. The sample with 30 wt % MA displayed excellent strength and high modulus comparable with typical amorphous plastics, and could be used as the matrix for composite materials.

At the same MA loading, resins derived from AE-ESBO showed higher mechanical strength than those derived from AESBO. When MA loading was 10 wt %, relatively large modulus improvement of $\sim 90\%$ was achieved by replacing AESBO with AE-ESBO. When MA loading was 30 wt %, modulus increase from $1136 \pm 21 \text{ MPa}$ to $1452 \pm 28 \text{ MPa}$, which is about 30% improvement. Tensile strength also increased from 33.6 ± 0.3 to $37 \pm 1.5 \text{ MPa}$. Better elongation was achieved in AESBO systems.

CONCLUSIONS

Allyl double bonds were introduced into fatty esters of soybean oil through a ring-opening nucleophilic addition reaction of allyl alcohol and transesterification. The allyl fatty ester contains higher concentration of double bond than allyl triglyceride. After copolymerization at the presence of a peroxide free radical initiator with MA, much higher modulus, tensile strength and glass transition temperature were achieved at the expense of elongation. These resins also demonstrated higher gel content, lower swelling ratio in toluene than those of the resins derived from AESBO. Strongest resin (AE-ESBO-*co*-MA30 wt %) has modulus of $1452 \pm 28 \text{ MPa}$, tensile strength of $37 \pm 1.5 \text{ MPa}$, and elongation of $4.2 \pm 0.5\%$.

ACKNOWLEDGMENTS

This work is supported by the US Department of Agriculture grant (USDA-CSREES 2009-38924-19840).

REFERENCES

1. Croston, C. B.; Tubb, I. L.; Cowan, J. C.; Teeter, H. M., *JAOCs*, **1952**, 29, 331.
2. Eichwald, E., US Pat. 2,160,572, **1939**.
3. Ghodssi, S. M. A.; Petit, J.; Valot, H., *Bull. Soc. Chim. Fr.* **1970**, 4, 1461.
4. Turner, S. W.; Blewett, C. W. US Pat. 4,973,743, **1990**.
5. Ionescu, M.; Petrović, Z. S. Polymerization of Soybean Oil with Superacids, Soybean—Applications and Technology; Ng, T.-B., Eds.; InTech, **2011**.
6. Petrović, Z. S.; Ionescu, M. US Pat. 3,550,961, **1951**.
7. Refvik, M. D.; Larock, R. C.; Tian, Q. *JAOCs*, **1999**, 76, 93.
8. Petrovic, Z.; Guo, A.; Javni, I. US Pat. 6,107,433, **2000**.
9. Guo, A.; Cho, Y.-J.; Petrović, Z. S. *J. Polym. Sci. Part A: Polym. Chem.* **2000**, 38, 3900.
10. Zlatanić, A.; Petrović, Z. S.; Dušek, K. *Biomacromolecules* **2002**, 3, 1048.
11. Petrović, Z. S.; Lukić, M.; Zhang, W.; Shirley, W. Academy of Science and Arts of Serbian Republic, Scientific Sessions vol VII, Section of natural, Mathematical and Technical Sciences Vol. 4. Theoretical and Experimental Investigation of Nanomaterials. Banja Luka, **2005**, p 261.
12. Petrović, Z. S.; Zhang, W.; Javni, I. *Biomacromolecules* **2005**, 6, 713
13. Petrović, Z. S.; Guo, A.; Javni, I. In Natural Fibers, Polymers and Composites—Recent Advances, Wallenberger, F. T.; Weston, N. E., Eds; Kluwer Academic Publishers: Boston, Dordrecht, London, **2004**; pp 167.
14. Guo, A.; Demydov, D.; Zhang, W.; Petrović, Z. S. *J. Polym. Environ.* **2002**, 10, 49.
15. Xu, Y.; Petrović, Z. S.; Das, S.; Wilkes, G. L. *Polymer* **2008**, 49, 4248.
16. Borden, G. W.; Smith, O. W.; Trecker, D. J. US Pat. 4,025,477, **1977**.
17. Borden, G. W.; Smith, O. W.; Trecker, D. J. US Pat. 4,220,569, **1980**.
18. D'Alelio, G. F. US Pat. 3,676,398, **1972**.
19. Hodakowski, L. E.; Osborn, C. L.; Harris, E. B. US Pat. 4,119,640, **1978**.
20. Hodakowski, L. E.; Hess, L. G. US Pat. 4,118,405, **1978**.
21. Mahmood, M. H.; Nor, H. M.; Kifli, H.; Rahman, M. A.; Rafiei, A. *Nucl. Sci. J. Malays.* **1991**, 9, 95.
22. Trecker, D. J.; Borden, G. W.; Smith, O. W. US Pat. 3,931,075, **1976**.
23. Wool, R.; Kusefoglu, S.; Palmese, G.; Khot, S.; Zhao, R. US Pat. 6,121,398, **2000**.
24. Ackerman, J. F.; Weisfeld, J.; Savageau, R. G.; Beerli, G. US Pat. 3,673,140, **1972**.
25. Borden, G. W.; Smith, O. W.; Trecker, D. J. US Pat. 3,876,518, **1975**.
26. Luo, Q.; Liu, M.; Xu, Y.; Ionescu, M.; Petrović, Z. S., *Macromolecules* **2011**, 44, 7149.
27. Paquot, C.; Hautfenne, A. Standard Methods for the Analysis of Oils, Fats and Derivatives; Blackwell Scientific: London, **1987**, pp 118–119.
28. Paquot, C.; Hautfenne, A. Standard Methods for the Analysis of Oils, Fats and Derivatives; Blackwell Scientific: London, **1987**, pp 88–93.
29. Smith, B. C. Infrared Spectral Interpretation: A Systematic Approach; CRC Press LLC, **1998**.
30. Sacristan, M.; Ronda, J.C.; Galia, M.; Cadiz, V. *Biomacromolecules* **2009**, 10, 2678.
31. Biswas, A.; Adhvaryu, A.; Gordon, S. H.; Erhan, S. Z.; Willett, J. L.; *J. Agric. Food Chem.* **2005**, 53, 9485.
32. Odian, G. Principles of Polymerization, 4th ed.; Wiley: Hoboken, New Jersey, **2004**.
33. Liu, H.; Wilén, C. E. *Macromolecules* **2001**, 34, 5067.